Heating characteristics of western hemlock (*Tsuga heterophylla*) in a high frequency field

Ciprian Lazarescu · Stavros Avramidis

Abstract The research aimed to establish whether dielectric heating of wood at high frequency could be accomplished fast, without excessive temperature fluctuations and no wood degrade. The intention was to develop optimized dielectric heating schedules in order to effectively pasteurize green timbers and logs for export—an eco-friendly substitute to currently used toxic chemical method. Data analysis revealed that the electric field distribution within the specimen was a strong function of its dielectric properties. Specifically, homogeneous moisture contents generated constant electric field values while heterogeneous distributions generated sudden drops and raises of the electric field strength with heating uniformly dispersed due to a fast redistribution from hot to colder areas. Convection losses through air contact may reduce the average heating rate of the timber shell by about 50%.

Verhalten von Western Hemlock (*Tsuga heterophylla*) bei Hochfrequenzerhitzung

Zusammenfassung In dieser Studie wurde untersucht, ob Hochfrequenzerhitzung von Holz schnell und ohne übermäßige Temperaturschwankungen und ohne Beeinträchtigung der Holzqualität durchgeführt werden kann. Ziel war es, ein optimiertes Erhitzungsprogramm zur effektiven phytosanitären Behandlung von für den Export bestimmtem Schnitt- und Rundholz zu entwickeln – als umweltfreundliche Alternative zu den gegenwärtig verwendeten toxischen chemischen Verfahren. Die Versuchsergebnisse zeigten, dass die Verteilung des elektrischen Feldes im Prüfkörper stark von dessen dielektrischen Eigenschaften abhing. Eine homogene Holzfeuchte ergab konstante elektrische Feldwerte. Eine heterogene Holzfeuchteverteilung führte zu plötzlichen Ab- und Anstiegen der elektrischen Feldstärke, jedoch wegen einer schnellen Umverteilung zwischen heißen und kalten Bereichen zu einer gleichmäßigen Aufheizung. Wärmeverluste durch Luftkontakt können die mittlere Aufheizrate der Schnittholzoberfläche um bis zu 50 % verringern.

1 Introduction

Dielectric heating of wood at high frequencies (*HF*) is potentially the most favourable pasteurization (phytosanitation) method for timbers and logs that are internationally traded in green condition (Lazarescu et al. 2009, 2010). This method is more eco-friendly compared to using toxic chemicals such as methyl bromide, and faster and gentler compared to using live steam.

HF by definition comprises both microwaves and radio waves. Microwaves contain a great deal of energy that could rapidly raise the temperature of a moist material, but microwaves experience small depths of penetration thus limiting wood volume heated simultaneously (not effective in batch situations) and standing waves that can result in cold spots (Constant et al. 1996). On the other hand, owing to their large wave lengths, radio waves can penetrate large volumes of material and since they contain lower energy amounts, they allow for a gentler but still swift temperature rise (Resch 2006). Furthermore, they are ideal for batch processing conditions (Avramidis et al. 1994; Elustondo et al. 2005).

A common problem encountered in radio frequency (*RF*) heating is the non-uniformity of the electromagnetic field inside the pasteurized material (Jiao et al. 2010; Johnson et al.

C. Lazarescu · S. Avramidis (✉)
Department of Wood Science, The University of British Columbia, 2424 Main Mall, Vancouver, BC V6T 1Z4, Canada
e-mail: stavros.avramidis@ubc.ca

Fig. 1 (**a**) *RFV* kiln, (**b**) structure of the heating assembly: *1*—FISO sensors, *2*—kiln dry insulating boards (13% *MC*) and (**c**) lengthwise position of the cross section where the sensors were placed
Abb. 1
(**a**) Hochfrequenzeinrichtung, (**b**) Aufbau der Heizeinheit: *1* – FISO-Sensoren, *2* – Isolierplatten (13 % Holzfeuchte) und (**c**) Längsposition des Querschnitts, an der die Sensoren platziert wurden
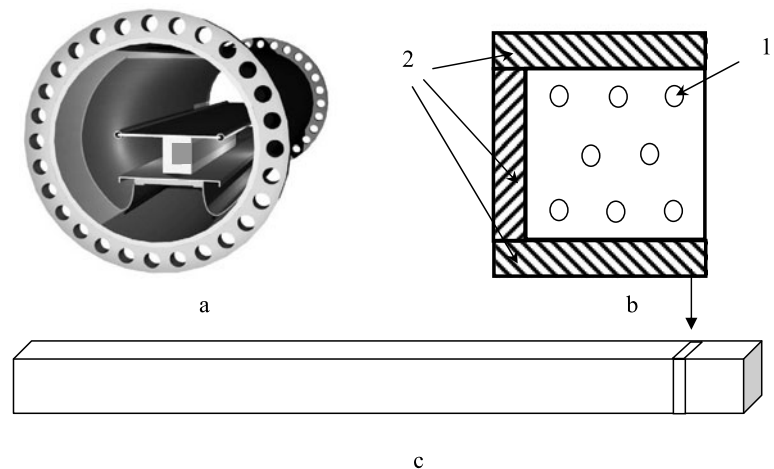
2010) that might result in uneven material heating. Wood is particularly susceptible to this situation because of the heterogeneous moisture distribution coupled with a complex chemical make up. This disadvantage could compromise the acceptance of *RF* heating as an eco-friendly alternative pasteurization method.

Western hemlock (*Tsuga heterophylla*) forests remain an important part of British Columbia's annual timber production and, with the new strategies of breaking the pine-forests into smaller patch mosaics of species (to avoid the rapid spread of a pest characteristic to one species) the production of hemlock lumber will become even more significant. Furthermore, temperate rainforest timbers like hemlock are an important global source of high quality fiber and one of the most important export species and one of the first on a "need to pasteurize" list. Therefore, this study assessed the *RF* heating of western hemlock for a wide variety of moisture content distributions and power densities under a single specimen configuration.

2 Materials and methods

Twenty, 2-m-long sound and green hemlock timbers having a cross section of 114×114 mm were obtained from a local sawmill. Prior to testing, they were submerged into water for one month so that the evaluation could start high moisture content (*MC*) specimens.

RF heating was carried out in a small (0.25 m^3) experimental *RFV* dryer (Avramidis et al. 1994; Lazarescu et al. 2009). The *RF* energy, produced by a solid-state generator, was directed to the upper electrode through a coaxial cable and an oscilloscope and a capacitor divider probe with known calibration was used to measure *RF* voltage values inside the heating area (Fig. 1a).

Timber temperature was continuously monitored, within the same plane (Fig. 1c), by eight fiber optic sensors (probes)

connected to a universal multichannel signal conditioning instrument (FISO UMI Technologies Inc., Quebec, Canada). All sensors were placed on the same vertical plane because of *MC* variability across timber width/thickness and since the electric field is highly influenced by it, its mapping allows more accurate simulations. In order to reduce the heating losses each timber was insulated using wood boards from the same species at about 13% *MC*, around three faces (Fig. 1b). Besides reducing surface heating losses, an increase in the electric field strength inside the specimen was expected due to the poor dielectric properties of the surrounding dry wood. One specimen side was left non-insulated for comparison purposes.

Five heating runs were conducted for each timber, the difference between them being *MC* (timbers were kept in a dry environment for two weeks before another run) and the length of the specimen that was reduced by 150 mm upon completion of each run. Length was reduced because post-heating evaluations included cutting samples around the areas where the sensors were fixed and *MC* measurements by ASTM D 1576 (oven-dry method). This allowed studying the effect of *MC* distribution over similar cross sections. Furthermore, the smaller volume from run-to-run resulted in higher power densities (kW/m^3)—full power of the generator (1000 W) was drawn for each run. A total number of 100 tests were carried out using this approach.

2.1 Dielectric properties

Since the dielectric properties vary with the proportion of latewood (Norimoto et al. 1978), oven-dry content of glucose and lignin (Venkateswaran 1972) or even the amount of crystalline regions (Norimoto 1976), individual measurements (twenty) were done for each timber, from high *MC*s to oven-dry, by placing a rectangular wood sample ($116 \times 90 \times 35$ mm^3) in the capacitive section of a parallel resonant circuit (Lazarescu and Avramidis 2011). All dielectric coefficients were measured in either radial or tangential
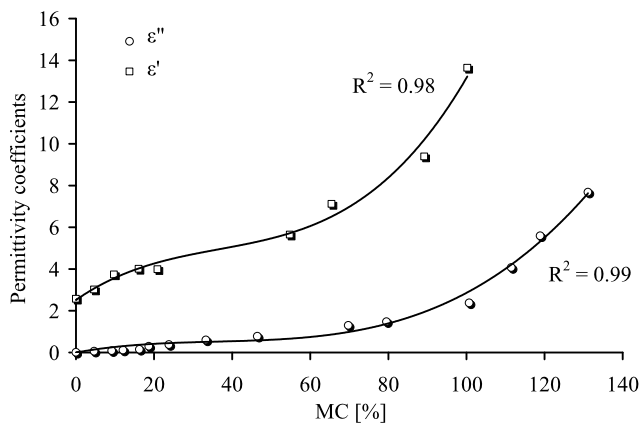
Fig. 2 Permittivity coefficients as a function of *MC*
Abb. 2 Dielektrizitätskoeffizienten in Abhängigkeit der Holzfeuchte (*MC*)
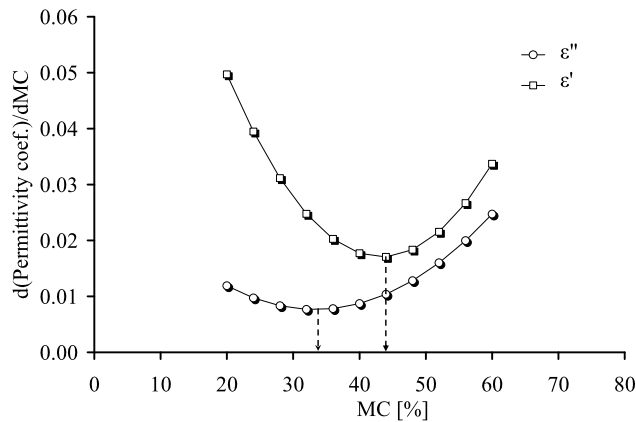

Fig. 3 Sample plots of the derivative of the imaginary (ε'') and real (ε') permittivity coefficients and how the *MC* associated with a change in slope was determined (*dotted arrow lines*)
Abb. 3 Beispiel zur Bestimmung der Holzfeuchte, bei der die Ableitung der imaginären (ε'') und realen (ε') Dielektrizitätskoeffizienten die Steigung ändert (*gestrichelte Pfeile*)

direction according to the position of the timber during the experiments inside the *RF* chamber. Both permittivity components (imaginary ε'' and real ε') were fitted with a third-degree polynomial (Fig. 2). Besides having high coefficients of determination, one of the main advantages of this type of fitting is that the derivative—a quadratic polynomial—allows easily determining the *MC* associated with a sudden change in dielectric properties (Fig. 3).

2.2 Power density calculations

The electric field value permeating the specimen was computed using Poisson Superfish, a set of programs designed to calculate electromagnetic fields in a 2-dimensional cavity that resonates at discrete frequencies (Halbach and Holsinger 1976). The frequency of the fundamental mode
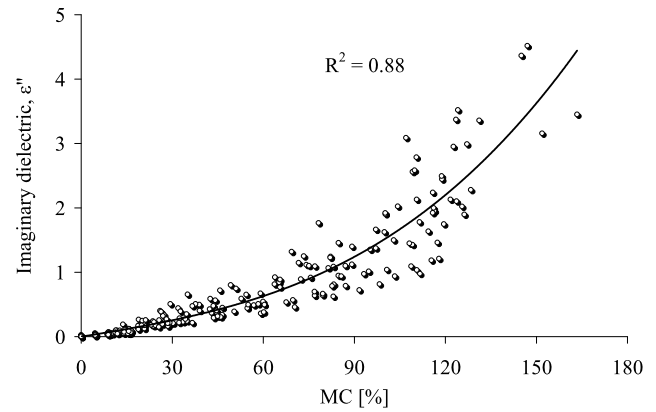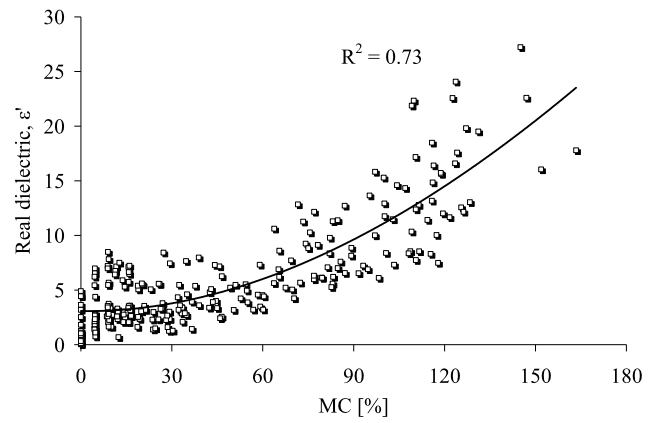
Fig. 4 Plots of real (*upper graph*) and imaginary dielectric coefficients versus *MC*
Abb. 4 Zusammenhang zwischen realen (*oberes Bild*) sowie imaginären Dielektrizitätskoeffizienten und der Holzfeuchte

was adjusted at 6.78 MHz by changing the permeability of a ferrite tuner. The electric field value for each subsection was used to measure the power deposited in the material (Torgovnikov 1993):
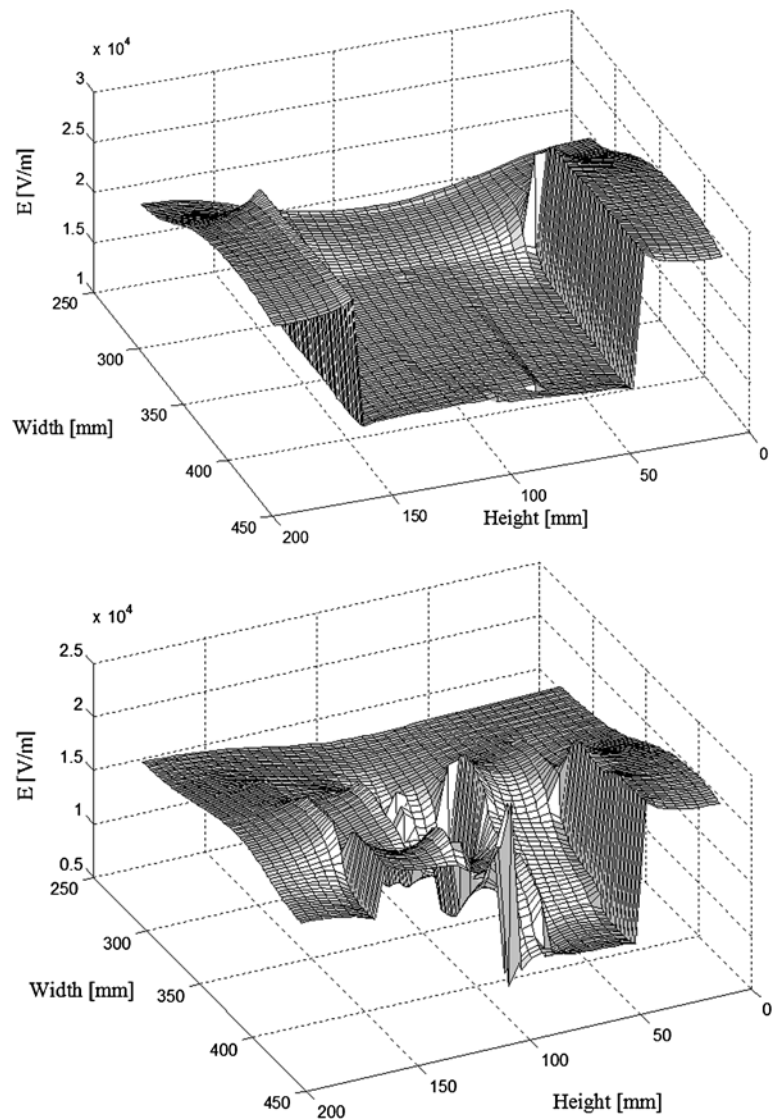
$$P_L = \pi f \varepsilon_0 \varepsilon'' \int_{V_L} |E|^2 dV_L \tag{1}$$

where P_L is the power loss, in W; f is the frequency, in MHz; ε_0 is the absolute permittivity of air, $\varepsilon_0 = 8.85 \times 10^{-12}$ F/m; E is the electric field, in V/m, and V_L is the volume, in m^3. Power density (P_D, in kW/m^3), another common way to express energy loss in dielectric processes, was computed by dividing power loss to the volume.

All experiments were performed at 1000 watts and all data were compared with the peak-to-peak "oscilloscope read" voltage value. These comparisons allowed measuring the generator—electrode losses that ranged between 3 and 8% and were later taken into account in computer simulations.

492

Eur. J. Wood Prod. (2012) 70:489–496

3 Results and discussion

3.1 Dielectric properties

Average *MC* values associated with a switch from a negative to a positive rate (graphically determined, see sample plots in Fig. 3) are close to fiber saturation point (*FSP*), namely, 27.94% (±7.07%) for imaginary (ε'') and 35.14% (±11.08%) for real (ε') permittivity coefficients. The imaginary coefficient, that is strongly related to the percentage of electric energy transferred to the material, showed a trend reversal from a decreasing to an increasing rate with the apparition of free water mainly due to the replacement of some air paths with more convective water layers (Torgovnikov 1993) or the increase in ionic conductivity (Skaar 1948). Higher *MC* trend reversal values were obtained for the real coefficient, which characterises the susceptibility to polarization, probably due to the higher bond energy (stronger bonds) of free water at moisture contents close to *FSP*. The weakening of the chemical links between cell wall and the free water existent in cell cavities, in this case at 35% *MC*, started the growing process in ε' values.

All 260 observations (13 measurements were done for each timber) collected during this phase were statistically analysed using a SAS/STAT® procedure that initially scrutinizes the significance of each variable in the presence of all the other variables and continues by "step-wise" dropping the ones having *F*-values below the 0.05 significance level (Fig. 4). A "non-intercept" model was favoured for the imaginary coefficient where the relationship between *MC*, in %, and the real and imaginary dielectric coefficients were:

$$\varepsilon' = 7.91 \times 10^{-4} MC^2 + 3.09, \qquad R^2 = 0.73 \qquad (2)$$

$$\varepsilon'' = 7.25 \times 10^{-7} MC^3 + 7.9 \times 10^{-3} \times MC,$$

$$R^2 = 0.88 \qquad (3)$$

Fig. 6 Influence of *MC* distribution (numbers in % inside the graph) over the electric field in a homogeneous (upper graph) and a heterogeneous *MC* timber
Abb. 6 Einfluss der Holzfeuchteverteilung (in Prozent angegeben im Diagramm) auf das elektrische Feld in einem Schnittholz mit homogener (*Bild oben*) und heterogener Holzfeuchteverteilung
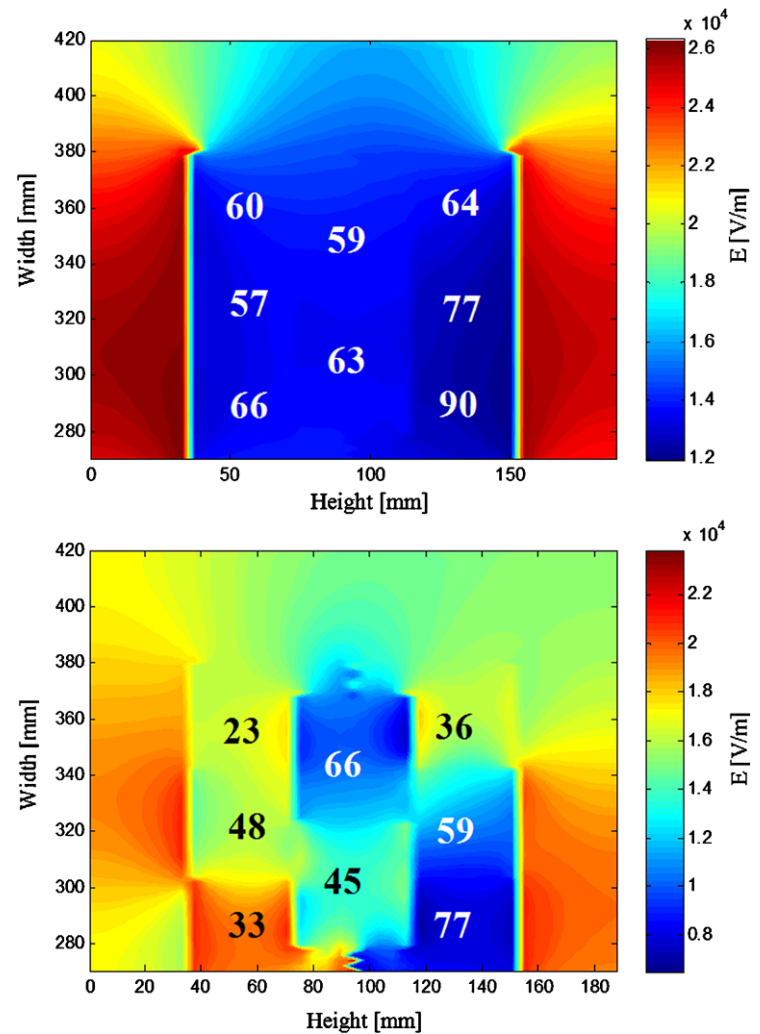

The intercept value for ε' which characterises the real dielectric coefficient at oven-dry values is similar to the value obtained by Salas et al. (1994) or to the value for MHz frequency dielectric fields—$\varepsilon'(0) = 3$—given by USDA (1999). That the imaginary dielectric coefficient was best fitted using an incomplete third degree polynomial slightly contradicts the findings of other researchers (Peyskens et al. 1984; Zhou and Avramidis 1999) who considered that a second degree polynomial describes better the physical relationship. The difference could lay in the accuracy of the readings, sample size or moisture content range, from 0 to 160% in this case, compared with smaller ranges in the other studies. The residuals that resulted from fitting at *MC* values over *FSP* increased in size (conical-shaped) giving a biased estimate of the standard deviation. This effect may be attributed to free water distribution, but could also be a consequence of differences in cellulose content, percentage of latewood or the presence of irregular arrays of cells (Norimoto et al. 1971).

3.2 Electric field distribution

The distribution of the electric field inside each specimen was a strong function of the dielectric properties of the wood itself. 3D plots of the electric field along the height and the width of a wood assembly having either a homogeneous or a heterogeneous moisture content distribution are shown in Fig. 5. The former have a more uniform electric field and therefore a more uniform heating rate might be expected. However, a different condition applies to the variable *MC* timber where the interaction between different dielectric coefficients generates sudden drops and raises of the electric field value (Fig. 6) thus resulting in cold spots and longer heating times.

This method might be used to map *MC* distributions based on electrical field readings where sudden drops in the electric field value will expose the presence of a wet pocket, for western hemlock or simply a heterogeneous moisture content distribution after the drying process, namely, core versus shell.

Fig. 7 Average P_D (in kW/m³)
increase within each *MC* class
Abb. 7 Mittlerer Anstieg der
Leistungsdichte P_D (in kW/m³)
mit ansteigender Holzfeuchte
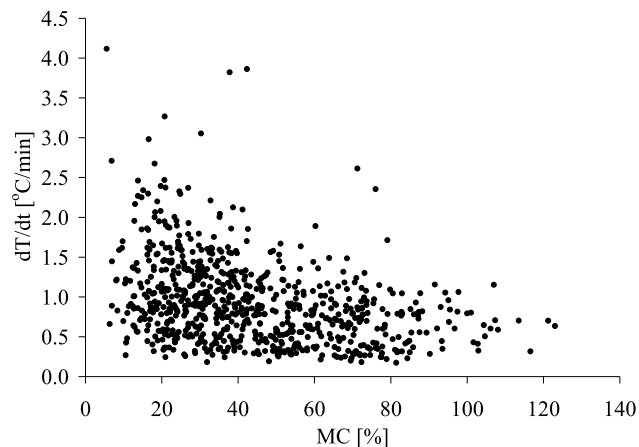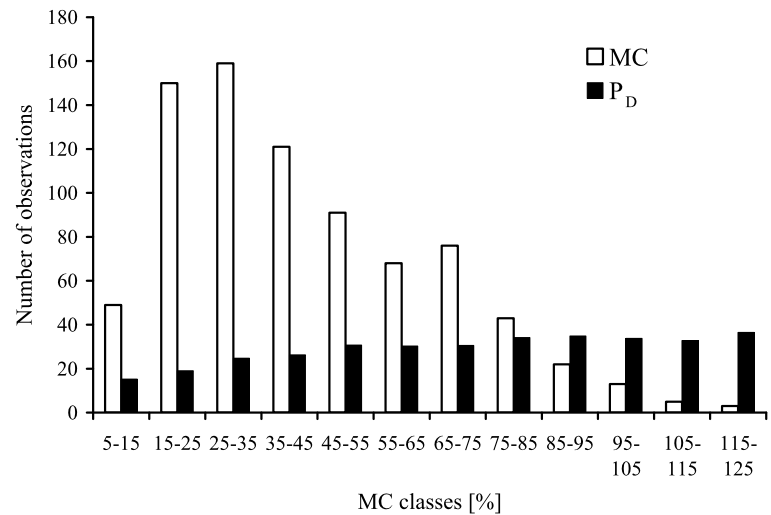
Fig. 8 dT/dt versus *MC* for all experiments
Abb. 8 Aufheizrate dT/dt in Abhängigkeit der Holzfeuchte bei allen
Versuchen
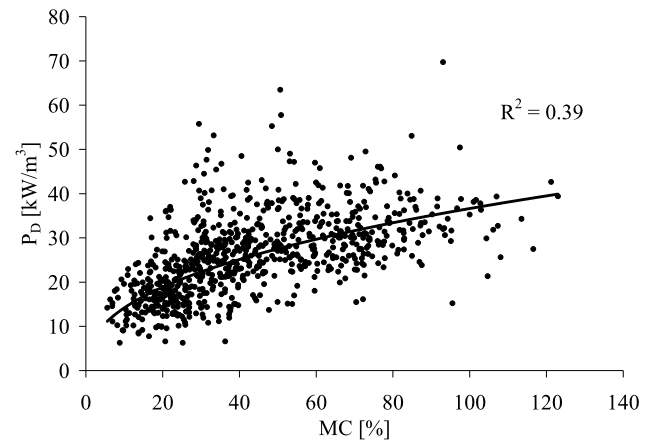
Fig. 9 P_D versus *MC* for all experiments
Abb. 9 Leistungsdichte P_D in Abhängigkeit der Holzfeuchte bei allen
Versuchen

The electrode voltage readings dropped during heating by about 18 to 25% in every run as a consequence of temperature increases indicating that the material became more "lossy" (higher ε'' values). Based on voltage drop measurements, a temperature raise of 10°C (initial temperature 20°C) resulted in an increase of the loss factor with 4.5% up to 6.25%, results comparable with the ones obtained for the same wood species by Zhou and Avramidis (1999). For the same temperature interval the specific heat of wood is expected to increase at about 3% per 10°C (USDA 1999) which roughly cancels out the increase of the loss factor. Average P_D increase within each *MC* class is illustrated in Fig. 7.

3.3 Heating rates

A number of 800 heating rates (dT/dt) and *MC* values were collected. Figure 8 reveals that dT/dt is not highly correlated
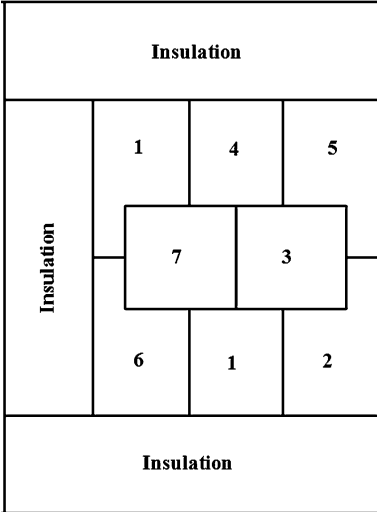
with *MC*—an important finding that underlines the versatile effect of *RF*-heating, namely, more power is absorbed by the areas in need (with higher moisture contents) and thus the heat is uniformly redistributed. The correlation between P_D and *MC* (Fig. 9) is derived using the following relationship:

$$P_D = 5.47 \times MC^{0.41}, \qquad R^2 = 0.39 \qquad (4)$$

Table 1 shows the distribution of the main variables measured during the heating, specifically, *MC*, P_D and dT/dt. Both minimum and maximum values of dT/dt were lower in areas 5 and 2 compared with the other locations because of convective losses to air. The plot of heating rate classes in all observations (Fig. 10) demonstrates a positive skew distribution with the interval 0.75 to 0.95 showing the highest number of observations. Only four recorded observations exhibited very high dT/dt of 3.15 to 4.15°C/min.

Eur. J. Wood Prod. (2012) 70:489–496

495

Table 1 MC, P_D and dT/dt distribution inside the tested wood block
Tab. 1 Verteilung der Holzfeuchte (MC), Leistungsdichte (P_D) und Aufheizrate (dT/dt) im Prüfkörper

Specimen assembly	Area #	MC, in %	P_D, in kW/m^3	dT/dt, in °C/min
	Area 1	6–121	10.2–50.4	0.24–4.12
	Area 2	8–117	10.2–63.5	0.18–1.89
	Area 3	10–123	8.6–47.0	0.27–3.86
	Area 4	6–92	10.3–49.9	0.45–3.82
	Area 5	11–90	9.8–57.7	0.17–1.37
	Area 6	9–97	8.4–69.7	0.35–2.37
	Area 7	9–108	6.3–49.0	0.28–2.98
	Area 8	7–85	6.3–53.1	0.42–2.47

Fig. 10 dT/dt class distribution
Abb. 10 Verteilung der Aufheizrate
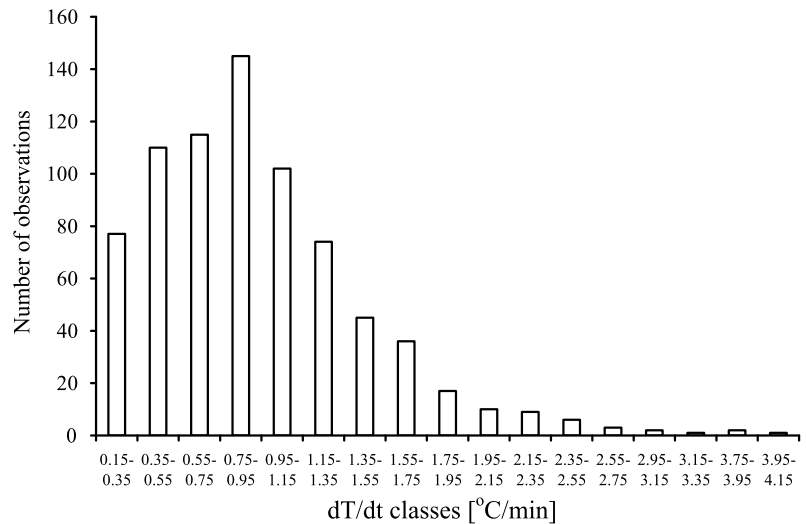
Covariance analysis of the two types of structural positions inside the tested timbers, interior areas #1, 3, 4, 6 and 8 and exterior areas #2 and 5, showed that the interaction between dT/dt and structural position is significant at the 0.05 level. A *post hoc* statistical test (Bonferroni multiple comparison) indicated that the two means were significantly different: interior (1.08°C/min) and exterior (0.50°C/min).

4 Conclusion

In the light of this investigation, the following conclusions are drawn:

(1) Changes in the imaginary permittivity coefficient rate are strongly associated with the transition from free to bound water (∼28% moisture content) while higher numbers were obtained for the real coefficient (∼35%).

(2) The distribution of the electric field inside the wood assembly was a strong function of the dielectric properties of the wet timber where homogeneous moisture contents generated constant electric field values while heterogeneous distributions generated sudden drops and raises of the electric field value.

(3) For this type of experimental design—several sensors located in the same cross section having a known moisture content distribution—the heating rates are not correlated with moisture content; this underlines the versatile effect of RF-heating which allows simultaneous rise of temperature within dry and wet areas;

(4) Convection losses through air contact may reduce the average heating rate of the shell with 50%.

References

Avramidis S, Liu F, Neilson BJ (1994) Radio-frequency/vacuum drying of softwoods: drying of thick western red cedar with constant electrode voltage. For Prod J 44(1):41–47

Constant T, Moyne C, Perré P (1996) Drying with internal heat generation: theoretical aspects and application to microwave heating. AIChE J 42(2):359–368

Elustondo D, Avramidis S, Zwick R (2005) The demonstration of increased lumber value using optimized lumber sorting and radio frequency vacuum drying. For Prod J 55(1):76–83

Halbach K, Holsinger RF (1976) Superfish—a computer program for evaluation of RF cavities with cylindrical symmetry. Part Accel 7:213–222

Jiao S, Tang J, Johnson JA, Tiwari G, Wang S (2010) Determining radio frequency heating uniformity in mixed beans for disinfestations. In: Proceedings of 2010 IMPI 44th annual microwave power symposium, 14–16 July 2010, Denver, Colorado, USA

Johnson JA, Wang S, Tang J (2010) Radio frequency treatments for insect disinfestation of dried legumes. In: Proceedings of 10th international working conference on stored product protection (IWC-SPP), June 27–July 2, 2010, Estoril, Portugal, 20 p

Lazarescu C, Avramidis S (2011) Radio—frequency heating kinetics of softwood logs. Dry Technol 29(6):673–681

Lazarescu C, Dale A, Uzunovic A, Breuil C, Avramidis S (2010) Radio frequency heating pasteurization of pine wood nematode (*Bursaphelenchus xylophilus*) infected wood. Eur J Wood Prod. doi:10.1007/s00107-010-0515-x

Lazarescu C, Plattner A, Hart F, Breuil C, Avramidis S (2009) Pasteurization of hemlock by radio frequency heating: a preliminary study. For Prod J 59(4):79–83

Norimoto M (1976) Dielectric properties of wood. Wood Res 59/60:106–152

Norimoto M, Hayashi S, Yamada T (1971) Anisotropy of dielectric constant in coniferous wood. Holzforschung 51:12–32

Norimoto M, Hayashi S, Yamada T (1978) Anisotropy of dielectric constant in coniferous wood. Holzforschung 32:167–172

Peyskens E, de Pourcq M, Stevens M, Schalck J (1984) Dielectric properties of softwood species at microwave frequencies. Wood Sci Technol 18(4):267–280

Resch H (2006) High-frequency electric current for drying of wood—historical perspectives. Maderas Cienc Tecnol 8(2):67–82

Salas WA, Ranson KJ, Rock BN, Smith KT (1994) Temporal and spatial variations in dielectric constant and water status of dominant forest species from New England. Remote Sens Environ 47:109–119

Skaar C (1948) The dielectric properties of wood at several radio frequencies. Technical publication Nr 69, New York State, Syracuse

Torgovnikov GI (1993) Dielectric properties of wood and wood-based materials. Springer, Berlin, 194 pp

USDA (1999) Wood handbook. Wood as an engineering material. US Dept agric. General technical report FPL-GTR-113, Chapter 3–22

Venkateswaran A (1972) A comparison of the electrical properties of milled wood, milled wood cellulose and milled wood lignin. Wood Sci 4(4):248–253

Zhou B, Avramidis S (1999) On the loss factor of wood during radio frequency heating. Wood Sci Technol 33(4):299–310